Biochimica et Biophysica Acta 1804 (2010) 56–62

Contents lists available at ScienceDirect

Biochimica et Biophysica Acta

journal homepage: www.elsevier.com/locate/bbapap

Review

Self-similar dynamics of proteins under hydrostatic pressure—Computer simulations and experiments

G.R. Kneller [a,b,c,*], V. Calandrini [a,c]

[a] Centre de Biophysique Moléculaire; Rue Charles Sadron; 45071 Orléans, France
[b] Université d'Orléans, UFR Sciences, BP 6759, 45067 Orléans, France
[c] Synchrotron Soleil; L'Orme de Merisiers, B.P. 48, 91192 Gif-sur-Yvette, France

ARTICLE INFO

Article history:
Received 26 March 2009
Received in revised form 5 May 2009
Accepted 29 May 2009
Available online 18 June 2009

Keywords:
Protein dynamics
Quasielastic neutron scattering
Hydrostatic pressure
Slow relaxation
Fractional Brownian dynamics

ABSTRACT

Different experimental techniques, such as kinetic studies of ligand binding and fluorescence correlation spectroscopy, have revealed that the diffusive, internal dynamics of proteins exhibits autosimilarity on the time scale from microseconds to hours. Computer simulations have demonstrated that this type of dynamics is already established on the much shorter nanosecond time scale, which is also covered by quasielastic neutron scattering experiments. The autosimilarity of protein dynamics is reflected in long-time memory effects in the underlying diffusion processes, which lead to a non-exponential decay of the observed time correlation functions. Fractional Brownian dynamics is an empirical model which is able to capture the essential aspects of internal protein dynamics. Here we give a brief introduction into the theory and show how the model can be used to interpret neutron scattering experiments and molecular dynamics simulation of proteins in solution under hydrostatic pressure.

1. Introduction

The dynamics of proteins is known to play an essential role for its function and the celebrated structure–function relationship has a counterpart in form of a dynamics–function relationship. In this context the thermodynamic and environmental conditions of a protein play an essential role. It has been demonstrated by Ferrand et al. that the functioning of bacteriorhodopsin (BR), which acts as a light-driven proton pump in the membrane of the archaebacterium *Halobacterium salinarum*, is strongly influenced by the temperature and the humidity of the membrane [1]. The study demonstrates that the function of BR is correlated with the presence of sufficiently large atomic position fluctuations. The latter are determined by the temperature and the flexibility, or "resilience", of the protein. As proposed by Zaccai, the latter may be modeled by an effective elastic force [2]. A corresponding simple model for the elastic incoherent structure factor has been used in a large number of elastic neutron scattering experiments, most of which were performed on hydrated protein powders. The presence of atomic position fluctuations implies atomic motion, but does not tell anything about the *time scale* of these motions. The spectrum of time scales for protein dynamics is extremely vast and ranges from sub-picoseconds to seconds and even hours. Quasielastic neutron can be used to probe the dynamics of proteins on the sub-picosecond to nanosecond time scale [3] and the upper end of the spectrum of time scales is covered by kinetic studies [4] and by fluorescence correlation spectroscopy [5,6]. The dynamics seen by all these techniques is essentially diffusive and the corresponding relaxation processes are characterized by non-exponentially decaying time correlation functions, which exhibit a power-law behavior for long times. Glöckle and Nonnenmacher have shown that the kinetics of ligand (re)binding in myoglobin, which reflects the internal dynamics of the protein, can be described by fractional Brownian dynamics (fBD) [7]. In contrast to normal Brownian dynamics, which is "memoryless" (Markovian), fBD displays long-time memory effects. To interpret their experiments with fluorescence correlation spectroscopy, Xie et al. describe the motion of a flavin fluorophore with respect to a nearby fluorescence-quenching tyrosine side chain by fractional Brownian dynamics in a harmonic potential [6,8–10], or, in technical terms, by a fractional Ornstein–Uhlenbeck (fOU) process. An overview on the theory of fractional kinetics and diffusion processes can be found in the review articles [11] and [12], respectively.

Molecular dynamics (MD) studies on lysozyme in solution have revealed that fBD is already developed on the pico- to nanosecond time scale [13], which is also accessible by quasielastic neutron scattering (QENS). A later article by one of us (GRK) shows in particular that the fOU process can be used to model QENS spectra from hydrated myoglobin powders obtained by Doster et al. [14]. From a physical point of view the fOU model is appealing since it combines a simple harmonic model describing the softness of a protein in terms of an effective force constant with a two-parameter model describing its relaxation dynamics. As pointed out in [13], fBD models can also be

* Corresponding author. Centre de Biophysique Moléculaire; Rue Charles Sadron; 45071 Orléans, France.
E-mail address: kneller@cnrs-orleans.fr (G.R. Kneller).

1570-9639/$ – see front matter © 2009 Elsevier B.V. All rights reserved.
doi:10.1016/j.bbapap.2009.05.007

linked to the theoretical framework of generalized Langevin equations, which has been developed in the 1960's by Zwanzig and Mori [15–18].

More recently we have used the fOU model to quantify the changes in the relaxation dynamics of lysozyme due to an external hydrostatic pressure, as seen by molecular dynamics simulations and quasielastic neutron scattering experiments [19–21]. Here the *changes* of the model parameters, rather than their absolute values were of interest. In the majority of experimental neutron scattering studies of protein dynamics the variation of the temperature has been used to gain insights into the structure of the protein energy landscape. The famous dynamical transition of proteins at temperatures of about 200K, which is often referred to as "glass transition", is the keyword in this context. In the early work of Doster et al. [14] the QENS spectra of myoglobin were interpreted on the basis of mode-coupling theory [22,23], which emphasizes the relation of slow protein dynamics to the relaxation dynamics of glasses [24]. Until now, pressure has been left largely unexplored as a thermodynamic parameter to study protein dynamics. Since a few years, however, the subject has regained the interest of several groups. We cite here studies by NMR [25], by neutron scattering [26,27], and by molecular dynamics simulations [28]. The study of proteins under pressure goes at least back to the work of Bridgeman in 1914 who observed that exerting pressure on egg white has a similar effect as boiling it [29]. A review on thermodynamic and biological studies of proteins under pressure can be found in an article by Balny et al. [30]. In order to extend the scope of such studies to include dynamical aspects it is necessary to reduce the number of parameters for the dynamical description of proteins to very few parameters. This corresponds very much to the transition from a microscopic, detailed description of condensed matter systems to equilibrium thermodynamics which describes these systems from a macroscopic point of view with very few parameters, such as temperature, pressure, volume etc. To achieve a similar goal for the description of protein relaxation dynamics, models based on fBD are a route to explore since they allow to make contact with simple physical models and to have at least a formal connection to a fully microscopic description of the dynamics. With the present article we try to give an introduction into the theory of fractional Brownian motion and show applications in relation with combined neutron scattering and MD simulation studies of proteins under hydrostatic pressure.

2. A model for protein dynamics

The internal dynamics of proteins probed by quasielastic neutron scattering is dominated by diffusive motions of the hydrogen atoms about their equilibrium positions. The reason is the dominating incoherent scattering cross section of hydrogen. The simple harmonic "resilience" model for proteins, which has shown its merits for the interpretation of elastic neutron scattering data [2], could be extended to describe QENS data by considering diffusive atomic motions in a harmonic potential. The corresponding stochastic process, the well-known Ornstein–Uhlenbeck (OU) process [31], leads, however, to an exponentially decaying position autocorrelation function which is not observed in reality [6]. The non-exponential relaxation dynamics of proteins can be accounted for by considering the *fractional* counterpart of the OU process which is discussed in the following. A detailed description for applications to neutron scattering can be found in [32] and we give here a compact presentation of the essential results, skipping mathematical derivations.

2.1. Fractional Ornstein–Uhlenbeck process

In general small step diffusion processes under the influence of an external force are described by Fokker–Planck equations, of which the Smoluchowski equation is a special case [33–35]. In the following we consider a generalization of the latter, which introduces a special type of long-time memory effects in the diffusion process. The time evolution of the probability $P(x,t|x_0, 0)$ for a displacement $x_0 \to x$ of a diffusing particle within a time t is then described by a fractional Smoluchowski (Fokker–Planck) equation [12],

$$\frac{\partial P(x,t|x_0,0)}{\partial t} = \tilde{\tau}^{1-\alpha}\,{}_0\mathcal{D}_t^{1-\alpha}\mathcal{L}P(x,t|x_0,0) \tag{1}$$

where $\mathcal{L}$ is the Smoluchowski operator

$$\mathcal{L} = D\frac{\partial}{\partial x}\left\{\frac{1}{k_B T}\frac{\partial V(x)}{\partial x} + \frac{\partial}{\partial x}\right\}. \tag{2}$$

Here D is a diffusion constant, $V(x)$ is the potential in which the particle moves, and k_B and T denote, respectively the Boltzmann constant and the absolute temperature. In the following we assume that $V(x)$ is harmonic, $V(x) = Kx^2/2$, with a positive force constant, K, and that it is sufficient to consider one-dimensional motions since the tagged atom moves in an isotropic (effective) potential. The symbol ${}_0D_t^{1-\alpha}$ defines a fractional derivative of order $1-\alpha$, which is defined through [36]

$${}_0\mathcal{D}_t^{1-\alpha} f(t) = \frac{d}{dt}\int_0^t d\tau \frac{(t-\tau)^{\alpha-1}}{\Gamma(\alpha)} f(\tau), \quad 0<\alpha\le 1. \tag{3}$$

Here $\Gamma(\cdot)$ is the Gamma function [37]. The constant $\tau\sim$ has the dimension of time and $\tau\sim^{1-\alpha}$ ensures thus the correct dimension of the r.h.s. of Eq. (1).

Defining the dimensionless variable $\xi = x/\sqrt{\langle x^2\rangle}$, where

$$\langle x^2\rangle = \frac{k_B T}{T} \tag{4}$$

is the mean square position fluctuation, the solution of Eq. (1) can be expressed in the form [12]

$$P(\xi,t|\xi_0,0) = \frac{\exp\left(-\frac{\xi^2}{2}\right)}{\sqrt{2\pi}}\sum_{n=0}^{\infty}\frac{1}{2^n n!}H_n\left(\frac{\xi_0}{\sqrt{2}}\right)H_n\left(\frac{\xi_0}{\sqrt{2}}\right)E_\alpha(-n\eta_\alpha t^\alpha). \tag{5}$$

The functions H_n are Hermite polynomials [37] and $E_\alpha(\cdot)$ is the Mittag-Leffler function, which has the series representation [38]

$$E_\alpha(z) = \sum_{k=0}^{\infty}\frac{z^k}{\Gamma(1+\alpha k)}. \tag{6}$$

The constant η_α is the fractional relaxation rate,

$$\eta_\alpha = \frac{D\tilde{\tau}^{1-\alpha}}{\langle x^2\rangle}. \tag{7}$$

The equilibrium distribution function is given by the long-time limit $P_{eq}(\xi) \equiv \lim_{t\to\infty} P(\xi, t|\xi_0, 0)$. In this limit only the term with $n=0$ survives in the series (Eq. 5) and $P_{eq}(\xi)$ has thus the same form as for the normal OU process, $P_{eq}(\xi) = \exp\left(-\frac{\xi^2}{2}\right)/\sqrt{2\pi}$. This implies that all equilibrium averages, such as the mean square position fluctuation, are left unchanged by the introduction of the fractional derivative in Eq. (1). For short times $P(\xi,t|\xi_0,0)$ approaches a Dirac distribution, $\lim_{t\to 0} P(\xi, t|\xi_0, 0)$, which is centered on the initial normalized position of the diffusing particle, ξ_0.

2.2. Time correlation functions and mean square displacement

The conditional probability density $P(\xi, t|\xi_0, 0)$ enables the calculation of time correlation functions. The position auto-

correlation function is for example obtained via $c_{xx}(t) \equiv \langle x(t)x(0)\rangle = \langle x^2\rangle \int\int d\xi d\xi_0 \xi\xi_0\ P(\xi,\ t|\xi_0,\ 0)\ P_{eq}(\xi_0)$,

$$c_{xx}(t) = \langle x^2\rangle E_\alpha(-\eta_\alpha t^\alpha), \tag{8}$$

and displays the algebraic decay for long times,

$$c_{xx}(t) \approx \frac{\langle x^2\rangle \eta_\alpha^{-1} t^{-\alpha}}{\Gamma(1-\alpha)}, \tag{9}$$

which is observed in experiments [39]. Similarly one obtains for the time-dependent mean square displacement (MSD)

$$W(t) = \langle [x(t)-x(0)]^2\rangle = 2\langle x^2\rangle(1 - E_\alpha(-\eta_\alpha t^\alpha)). \tag{10}$$

For short times the MSD has the form $W(t) \approx 2D_\alpha\, t^\alpha$ and displays "subdiffusive" behavior if $0<\alpha<1$. Here $D_\alpha = \langle x^2\rangle \eta_\alpha$ is the fractional short time diffusion coefficient. For $\alpha = 1$ the short time evolution of $W(t)$ exhibits normal Einstein diffusion, $W(t) \approx 2Dt$, where $D \equiv D_1$.

The function $E_\alpha(-t^\alpha)$ decays monotonously [38] and can be represented as a superposition of decaying exponential functions [7,32],

$$E_\alpha(-t^\alpha) = \int_0^\infty d\lambda p(\lambda) \exp(-\lambda t), \tag{11}$$

where $p(\lambda)$ is the relaxation rate spectrum

$$p(\lambda) = \frac{1}{\pi} \frac{\lambda^{\alpha-1}\sin(\pi\alpha)}{\lambda^{2\alpha} + 2\lambda^\alpha \cos(\pi\alpha) + 1}, \quad 0 < \alpha \le 1. \tag{12}$$

It follows from Eq. (11) that $E_\alpha(-t^\alpha)$ is the moment generating function of $p(\lambda)$ and since all derivatives of $E_\alpha(-t^\alpha)$ diverge at $t=0$, the moments of $p(\lambda)$ do not exist. One can, however, easily calculate the median, $\lambda_{1/2}$, of $p(\lambda)$, which is defined by $\int_0^{\lambda 1/2} d\lambda\ p(\lambda) = 1/2$. For $p(\lambda)$ as given by Eq. (12) $\lambda_{1/2}$ [40].

In the following we need also the Fourier transform of the function $E_\alpha(-t^\alpha)$,

$$L_\alpha(\omega) = \int_{-\infty}^{+\infty} d\omega \exp(-i\omega t) E_\alpha(-t^\alpha). \tag{13}$$

The "generalized Lorentzian" has the form [13]

$$L_\alpha(\omega) = \frac{2\sin(\alpha\pi/2)}{|\omega|(|\omega|^\alpha + 2\cos(\alpha\pi/2) + |\omega|^{-\alpha})}, \quad 0 < \alpha \le 1. \tag{14}$$

The calculation of neutron-related quantities can be found in [32], and we give here only the resumé. In the context of QENS experiments from biological macromolecules it is sufficient to consider incoherent scattering from the hydrogen atoms and we consider here the scattering from one single, "representative" atom. In this case the intermediate scattering function takes the form

$$I(q,t) = \exp\left(-q^2\langle x^2\rangle\right) \sum_{n=0}^{\infty} \frac{q^{2n}\langle x^2\rangle^n}{n!} E\alpha(-n\eta_\alpha t_\alpha). \tag{15}$$

The intermediate scattering function cannot be reduced to Gaussian form, except for $\alpha = 1$, where $I(q,\ t) = \exp(-q^2 W(t)/2)$. In contrast, the elastic incoherent structure factor (EISF), which is defined as the long-time limit of the intermediate scattering function, $\mathrm{EISF}(q) = \lim_{t\to\infty} I(q,\ t)$, does have Gaussian form,

$$\mathrm{EISF}(q) = \exp\left(-q^2\langle x^2\rangle\right), \tag{16}$$

independently of the value of α.

The dynamic structure factor is finally obtained by a Fourier transform of the intermediate scattering function,

$$S(q,\omega) = \frac{1}{2\pi}\int_{-\infty}^{+\infty} dt \exp(-i\omega t) I(q,t). \tag{17}$$

The Fourier transform can be performed combining Eqs. (14) and (15),

$$S(q,\omega) = \exp\left(-q^2\langle x^2\rangle\right)\left\{\delta(\omega) + \sum_{n=1}^{\infty} \frac{q^{2n}\langle x^2\rangle^n}{n!} \frac{\tau_{\alpha,n}}{2\pi} L_\alpha\left(\omega\tau_{\alpha,n}\right)\right\}. \tag{18}$$

Here we set

$$\tau_{\alpha,n} = (n\eta_\alpha)^{-1/\alpha}. \tag{19}$$

3. Protein dynamics under pressure by simulation and quasielastic neutron scattering

In the following we present results of molecular simulation and neutron scattering studies on lysozyme in solution under pressure, combining results from references [20] and [21].

3.1. Simulations

All simulations have been performed for a single lysozyme molecule in water confined in an orthorhombic simulation box, with dimensions $6.16\times4.19\times4.61$ nm^3 at ambient pressure. The coordinates for the starting configuration of lysozyme have been taken from entry 193L [41] of the Brookhaven Protein Data Bank [42], adding the positions of the hydrogen atoms by applying standard geometrical criteria. This leads to a total number of 1960 atoms for the lysozyme molecule. The simulation box was filled with 3403 water molecules, leading thus to a total number of 12,169 atoms for the simulated system.

The molecular dynamics simulations were performed with the MMTK simulation package [43], using the Amber94 force field [44], periodic boundary conditions and a velocity-Verlet integrator with a time step of 1 fs. All simulations were performed in the thermodynamic NpT-ensemble [45,46], fixing T to room temperature and varying the pressure from 0.1 MPa (1 bar) to 300 MPa (3 kbar). Here only simulations at 0.1 MPa and 300 MPa are reported on. For both pressures we created a short trajectory of 20 ps, with a sampling time step of $\Delta t = 0.005$ ps, and a long trajectory of 1 ns, with a sampling time step of $\Delta t = 0.04$ ps. The short and long trajectories were used to examine the fast and slow dynamics, respectively. In the first case we concentrated on high-frequency motions in a relatively short time window and in the second case on slow, collective motions which occur on longer time scales and which can be sampled at a lower rate. Prior to all analyses, the global translational and rotational motions of the lysozyme molecule have been removed. For this purpose we used a quaternion-based superposition algorithm [47,48] in order to superpose all protein configurations along a given trajectory with the corresponding initial configuration.

3.2. Neutron scattering experiments

The experiments were performed on deuterated solutions at a concentration of 60 mg/ml and a pD of 4.6, which was chosen as a compromise to obtain an exploitable concentration for neutron scattering experiments and to avoid, on the other hand, aggregation of the lysozyme molecules. The absence of aggregation was checked by small angle neutron scattering. We quote in this context light scattering experiments on lysozyme in solution [49] and small angle neutron scattering experiments [50] which have shown that aggregation does not occur up to concentrations of 100 mg/ml.

The QENS experiments were performed on the time-of-flight spectrometer IN5 at the Institut Laue-Langevin in Grenoble, using an incident neutron wavelength of $\lambda = 0.5$ nm and an elastic q-range of 3–23 nm^{-1}. The strong scattering by the pressure cell was subtracted. Moreover, the QENS data were corrected for detector efficiency, normalized to the integrated vanadium intensity, and mapped onto a (q, w) grid, where w and q are, respectively, the energy and momentum transfer in units of $\hbar$. More details on the experimental setup and the pressure cell can be found in refs. [21] and [51].

3.3. Results

The time-dependent mean square displacement is the fundamental quantity to be analyzed in the study of diffusive motions. Fig. 1 shows the simulated average MSD of the hydrogen atoms in lysozyme, which is due to internal protein dynamics. The labels "fast" and "slow" refer to the fast and slow dynamical regimes, respectively. In the first case the MSDs are systematically smaller since the configuration space is insufficiently sampled. As expected, pressure leads to a reduction of the motional amplitudes. One observes for both pressures and both trajectories excellent fits for the model of a fractional Ornstein–Uhlenbeck process. Here the mean square position fluctuation has been fixed to the values which have been directly calculated from the corresponding MD trajectories. The parameter α is not significantly influenced by pressure and stays close to 0.5 for the long trajectory and close to 0.6 for the short one. The evolution of the parameter τ with pressure shows inverse tendencies for the two dynamical regimes: with regards to the slow dynamics, τ is slightly increased, whereas it is reduced for the fast dynamics. The analysis of the intermediate scattering function presented below will confirm these results. For the slow dynamical regime at ambient pressure we show for comparison also the fit for the model MSD in case of a normal Ornstein–Uhlenbeck process (corresponding to $\alpha = 1$), which demonstrates that exponential relaxation is inappropriate to describe protein relaxation dynamics.

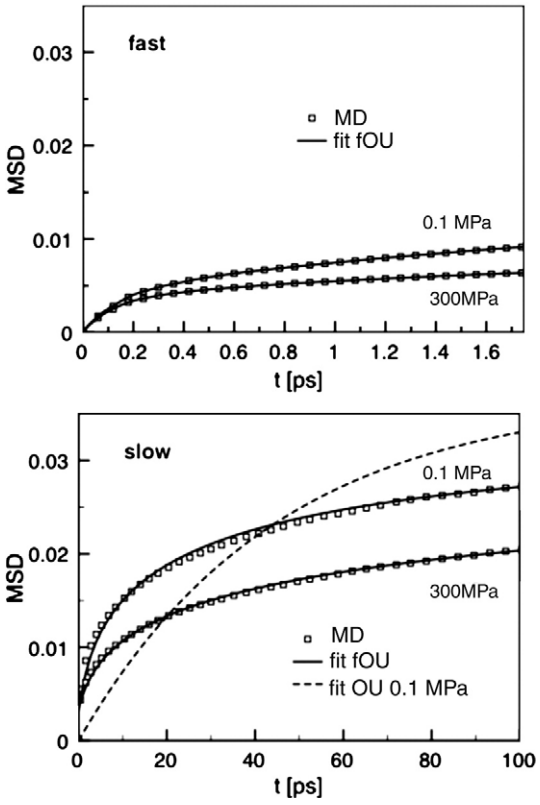

Fig. 1. Simulated average mean square displacement of the hydrogen atoms in lysozyme under hydrostatic pressure (squares). Global motions of the lysozyme molecule have been subtracted. The labels "fast" and "slow" refer to the fast and slow dynamical regimes, respectively. The panels show also the fits of the fOU model (solid line) and, for comparison, a fit of the OU model for the slow regime (broken line). The data have been taken from Ref. [21].

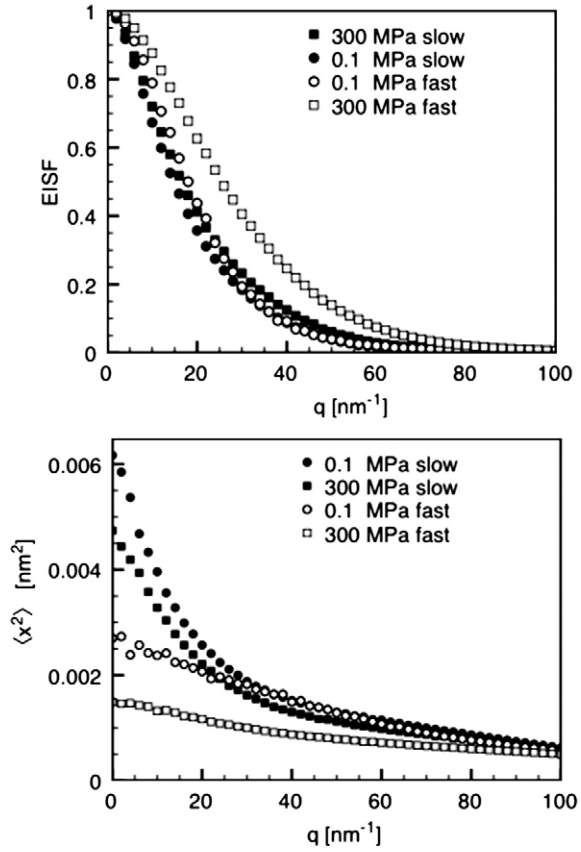

Fig. 2. Top: simulated EISF of lysozyme under pressure for the fast and slow dynamical regimes, respectively. Bottom: corresponding mean square position fluctuation as a function of q, defined according to Eq. (20). The data have been taken from Ref. [21].

A more detailed, space resolved analysis of the diffusive motions in lysozyme can be obtained through the simulated incoherent intermediate scattering function. In this context it must be emphasized that the EISF of the fOU model is Gaussian in q, which does not correspond to reality, since the different hydrogen atoms in a protein perform motions of different amplitudes and, even if the EISF of an individual atom is Gaussian, this is not anymore true for the total EISF (see Fig. 2, upper panel). As proposed in [52], the EISF can be modeled as a superposition of Gaussians, $\mathrm{EISF}(q) = \int_0^\infty d\langle x^2\rangle w(\langle x^2\rangle)\exp(-q^2\langle x^2\rangle)$, where $w(.)$ is an appropriate distribution function. Concerning the fOU model, this leads simply to a q-dependence of the model parameters, and concerning the mean square position fluctuation we write formally

$$\mathrm{EISF}(q) + \exp\left(-q^2\langle x^2\rangle(q)\right). \tag{20}$$

The simulated EISF can now be used to define a q-dependent mean square position fluctuation in the fOU model for $I(q, t)$ (see lower panel of Fig. 2).

Fig. 3 displays the simulated incoherent intermediate scattering function of lysozyme for the two dynamical regimes together with the fit of the fOU model. Here up to 12 terms of the series (Eq. 15) have been used and the mean square position fluctuation has been fixed according to definition (Eq. 20). Fig. 4 show the experimental data for the dynamic structure factor at the same q-value. In contrast to analyses of simulation data, the treatment of experimental QENS spectra does

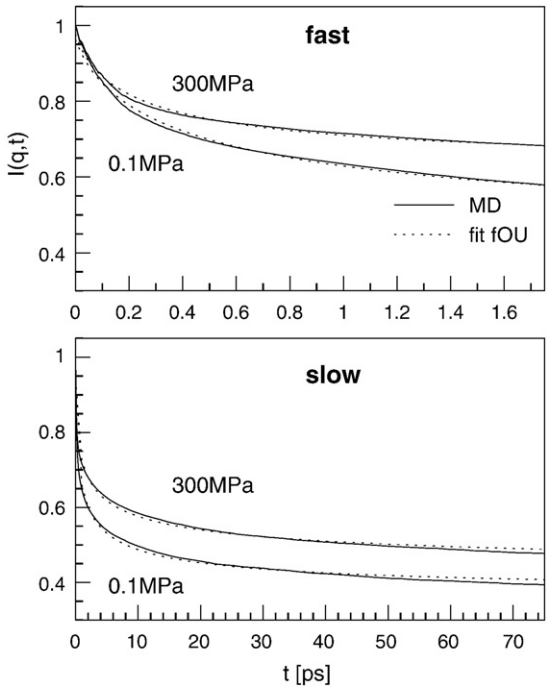

Fig. 3. Simulated incoherent intermediate scattering function of lysozyme under pressure for $q=20$ nm^{-1} corresponding to the fast and slow dynamical regimes, respectively (dots). The fits of the fOU model (Eq. 15) are shown as solid lines. The data have been taken from Ref. [21].

not allow to subtract rigid-body motions of proteins directly from the experimental data. They must thus be explicitly accounted for in the model, together with finite instrumental resolution,

$$S_m(q,t) = (S*l*r)(\omega). \tag{21}$$

Here S is given by Eq. (18), $l(\omega)=(1/\pi)Dq^2/([Dq^2]^2+\omega^2)$ is a Lorentzian for global translational diffusion, with D being the diffusion coefficient, and $r(.)$ the resolution function. We assumed the latter to be a Gaussian. The rotational diffusional motion of lysozyme can be neglected in the model since it is too slow to be detected with the available spectrometer. Concerning the internal dynamics, the mean square position fluctuation has been fixed according to Eq. (20), using the simulated EISF. In addition to the fit of the fOU model for the data at 300 MPa we show a fit with $\alpha=1$ (normal Ornstein–Uhlenbeck (OU) model). As for the MSD, the result illustrates nicely that the relaxation processes are non-exponential. Although the available frequency window is quite small, one observes that the decay of the experimental spectrum with w is roughly proportional to $w^{-3/2}$ and not proportional to w^{-2}, as for a normal Lorentzian (see Eq. (14)). The above difference in the high-frequency part of the QENS spectra is displayed by the fOU model and the OU model, respectively, if only the term $n=1$ in the series (Eq. 18) is taken into account. We remark that the effects of resolution and translational diffusion can be neglected at high frequencies. It should be noted that, although the experimental data scatter considerably at $w>1$ THz, the fit of the OU model is systematically below the experimental data.

It should be mentioned that the quasielastic broadening of the neutron scattering spectrum for q-values below 18 nm^{-1} is too small to allow for a statistically significant analysis. In this context we note also that the signal from the dynamics of a protein in solution contributes only for a few percent to the total scattering intensity. We analyzed finally only the QENS spectra at $q=20$ nm^{-1} and $q=22$ nm^{-1} since at higher q-values we were limited by the available q-range of 3–23 nm^{-1}.

From the fit of Eq. (21) we find for the translational diffusion constant $D=0.53(3)\ 10^{-4}$ nm^2/ps at ambient pressure and $D=0.50\ (3)\cdot 10^{-4}$ nm^2/ps at 300 MPa. These values can be compared with results from light scattering experiments by Nystrøm and Roots [49], which have been performed in similar conditions. They find $D=1.45\cdot 10^{-4}$ nm^2/ps and $D=1.25)\cdot 10^{-4}$ nm^2/ps at $p=0.1$ MPa and $p=300$ MPa, respectively.

The fit parameters of the fOU model corresponding to the simulated incoherent intermediate scattering function are depicted in the upper and lower panels of Fig. 5, respectively. The values of α and τ for $q=0$ correspond to the mean square displacement. We report in addition the fit parameters α and τ corresponding to the

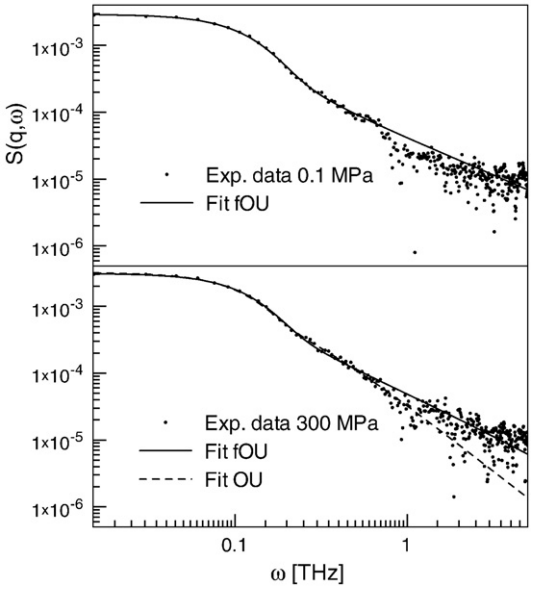

Fig. 4. Experimental dynamic structure factor of lysozyme under pressure for $q=20$ nm^{-1} (dots). The data have been obtained from the IN5 spectrometer of the Institut Laue-Langevin. Details are given in the text. The figure shows also the fits of the models fOU and OU (solid line and broken line, respectively), taking into account finite instrumental resolution and translational diffusion of the protein. The data have been taken from Ref. [20].

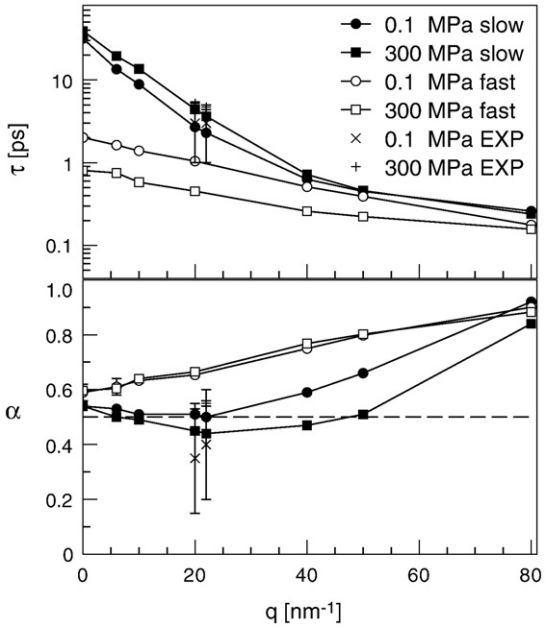

Fig. 5. Fit parameters τ (upper panel) and α (lower panel) of the fOU model for the simulated $I(q, t)$ and for the experimental dynamic structure factors. The data have been taken from Refs. [20] and [21].

experimental dynamic structure factor, together with the estimated errors. To understand the meaning of the q-dependence of τ and α it is helpful to introduce the van Hove correlation function [53], which is related to the intermediate scattering function via a spatial Fourier transform

$$I(q,t) = \int_{-\infty}^{+\infty} dq \exp(iqx) G(x,t). \quad (22)$$

The van Hove (self) correlation function gives the probability for a displacement x within a time span t,

$$G(x,t) = \langle \delta(x - [x(t) - x(0)]) \rangle. \quad (23)$$

Here the average has to be performed over all initial positions, $x(0)$, and all possible positions at time t, $x(t)$. For high q-values the van Hove function $G(x, t)$ contributes only substantially to the Fourier integral (Eq. 22) if it varies rapidly in space. This is the case for small times, knowing that $G(x, 0) = \delta(x)$. The intermediate scattering function for small values in q reflects, in contrast, *all* motions of the diffusing particle. Having this in mind, we see that τ decreases in general with the localization of the motions. At the same time α takes values closer to one, which means that the relaxation of localized motions is faster and more "Markovian" than the one of large amplitude motions. The increase of α with q is seen to be quite different for the short trajectory and the long one. In the first case α increases almost linearly, whereas it seems to go though a minimum for intermediate q-values in the second case, but a more refined analysis in q would be necessary to confirm this evolution. Concerning the influence of pressure, it appears first of all that the fast localized motions are accelerated, whereas the slow dynamics, involving large amplitude motions, is slowed down. This can be understood from the fact that large scale motions, which require spatial rearrangement of many atoms, are even more hindered under pressure than under normal conditions. The faster collision-type motions are, in contrast, accelerated since the mean free path is reduced under pressure. We remark also that for the fast dynamical regime τ is more influenced by pressure than α, whereas the contrary is true for the slow relaxation dynamics.

In the upper panel of Fig. 6 we show finally the relaxation rate spectrum for the MSD and in the lower panel the one for the intermediate scattering function. We consider here only the slow dynamical regime, which corresponds to the time scale of the QENS experiment. The relaxation rate spectrum of the latter is obtained by combining expressions in Eqs. (11), (12), and (15),

$$p_{\alpha,\tau,q}(\lambda) = \exp\left(-q^2\langle x^2\rangle\right)\left(\delta(\lambda) + \sum_{n=1}^{\infty} \frac{q^{2n}\langle x^2\rangle^n}{n!}\tau_{\alpha,n} p\left(\tau_{\alpha,n}\lambda\right)\right), \quad (24)$$

where $\tau_{\alpha,n}$ is given by Eq. (19). For both the MSD and the intermediate scattering function one observes a slight shift of the relaxation rate spectrum towards smaller relaxation rates, which is more pronounced in the second case. We attribute the latter property to the fact that the impact of pressure is particularly pronounced at intermediate values of q ($20\ \mathrm{nm}^{-1} < q < 50\ \mathrm{nm}^{-1}$) where α deviates most from one.

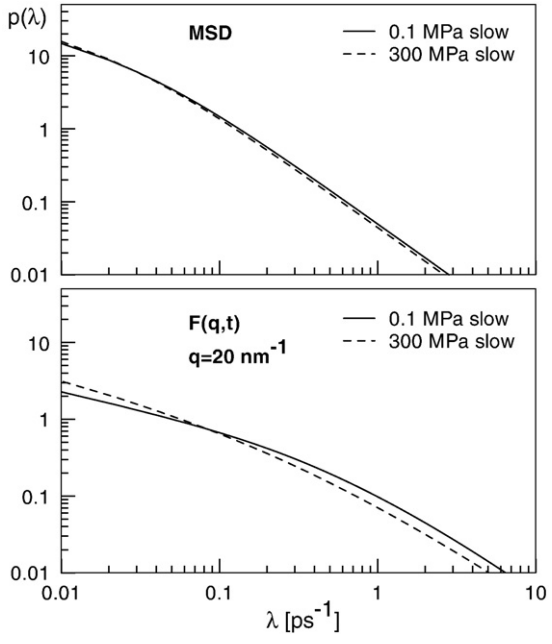

Fig. 6. Relaxation rate spectra for the simulated MSD (upper panel) and for $I(q, t)$ (lower panel), calculated for the slow dynamical regime.

4. Conclusion

In this article we have reviewed some recent studies of lysozyme under hydrostatic pressure, in which a combined simulation and experimental approach has been used. To analyze both simulation and experimental data we used the fractional Ornstein–Uhlenbeck process as a model for the motions of a tagged hydrogen atom in the protein. The model describes anomalous diffusion of a particle in an effective harmonic potential and extends the simple and successful harmonic "resilience" model proposed by Zaccai to the dynamical regime. The latter is described by a parameter τ, the inverse of which defines the median of a distribution of relaxation rates, and a parameter α, which expresses the deviation from normal Markovian diffusion. The power-law decay for the resulting correlation functions is characteristic for complex systems in general. The model links effectively the fast time scales explored by neutron scattering and MD simulations to the much longer time scales of functional motions. We have shown that the fractional Ornstein–Uhlenbeck process allows not only to represent the non-exponential relaxation dynamics of proteins, but is also appropriate to quantify the impact of pressure on the latter. We found in particular that pressure tends to accelerate fast and localized motions, whereas relaxation processes involving large amplitude motions are slowed down.

Our studies have also shown that a combined simulation and experimental approach is crucial for a successful analysis of QENS from proteins in solution. This analysis is very delicate since the signal from internal protein motions contributes only a few percent to the total spectrum, even if a deuterated solvent is used and only an "MD-guided" analysis of the data allows to appreciate details in the experimental data. We think that the proposed model can still be improved by introducing for example an analytical distribution for the mean square position fluctuations which can account for the motional heterogeneity of the hydrogen atoms.

Acknowledgements

Vania Calandrini acknowledges financial support from the French National Research Agency (Agence Nationale de la Recherche, contract ANR-06-CIS6-012-01).

References

[1] M. Ferrand, A. Dianoux, W. Petry, J. Zaccai, Thermal motions and function of bacteriorhodopsin in purple membranes: effects of temperature and hydration studied by neutron scattering, Proc. Natl. Acad. Sci. U.S.A. 90 (1993) 9668–9672.
[2] G. Zaccai, How soft is a protein? A protein dynamics force constant measured by neutron scattering, Science 288 (2000) 1604–1607.
[3] M. Bée, Quasielastic Neutron Scattering, Principles and Applications in Solid State Chemistry, Biology and Materials Science, Adam Hilger, Bristol, 1988.
[4] R.H. Austin, K.W. Beeson, L. Eisenstein, H. Frauenfelder, I.C. Gunsalus, Dynamics of ligand binding to myoglobin, Biochemistry 14 (1975) 5355–5373.
[5] H. Lu, L. Xun, S.X. Xie, Single molecule enzymatic dynamics, Science 282 (1998) 1877–1882.

[6] H. Yang, G. Luo, P. Karnchanaphanurach, T. Louie, I. Rech, S. Cova, L. Xun, X. Xie, Protein conformational dynamics probed by single-molecule electron transfer, Science 302 (5643) (2003) 262–266.
[7] W. Glöckle, T. Nonnenmacher, A fractional calculus approach to self-similar protein dynamics, Biophys. J. 68 (1995) 46–53.
[8] H. Yang, X. Xie, Probing single-molecule dynamics photon by photon, J. Chem. Phys. 117 (24) (2002) 10965–10979.
[9] S. Kou, X. Xie, Generalized Langevin equation with fractional Gaussian noise, Phys. Rev. Lett. 93 (2004) 180603.
[10] W. Min, G. Luo, B. Cherayil, S. Kou, X. Xie, Observation of a power-law memory kernel for fluctuations within a single molecule, Phys. Rev. Lett. 94 (2005) 198302.
[11] M. Shlesinger, G. Zaslavsky, J. Klafter, Strange kinetics, Nature 363 (1993) 31–37.
[12] R. Metzler, J. Klafter, The random walk's guide to anomalous diffusion: a fractional dynamics approach, Phys. Rep. 339 (2000) 1–77.
[13] G. Kneller, K. Hinsen, Fractional Brownian dynamics in proteins, J. Chem. Phys. 121 (20) (2004) 10278–10283.
[14] W. Doster, S. Cusack, W. Petry, Dynamical transition of myoglobin revealed by inelastic neutron scattering, Nature 337 (1989) 754–756.
[15] R. Zwanzig, Statistical Mechanics of Irreversibility, Lectures in Theoretical Physics, Wiley-Interscience, New York, 1961, pp. 106–141.
[16] H. Mori, A continued fraction representation of the time correlation functions, Prog. Theor. Phys. 34 (3) (1965) 399–416.
[17] J. Boon, S. Yip, Molecular Hydrodynamics, McGraw Hill, New York, USA, 1980.
[18] R. Zwanzig, Nonequilibrium Statistical Mechanics, Oxford University Press, Oxford, UK & New York USA, 2001.
[19] V. Hamon, P. Calligari, K. Hinsen, G. Kneller, Simulation studies of structural changes and relaxation processes in lysozyme under pressure, J. Non-Cryst. Solids 352 (2006) 4417–4423.
[20] V. Calandrini, G. Kneller, Influence of pressure on the fractional relaxation dynamics in proteins: a simulation study, J. Chem. Phys. 128 (6) (2008) 065102.
[21] V. Calandrini, V. Hamon, K. Hinsen, P. Calligari, M.-C. Bellissent-Funel, G. Kneller, Relaxation dynamics of lysozyme in solution under pressure: combining molecular dynamics simulations and quasielastic neutron scattering, Chem. Phys. 345 (2008) 289–297.
[22] W. Götze, M. Lücke, Dynamical current correlation functions of simple classical liquids for intermediate wave numbers, Phys. Rev. A 11 (6) (1975) 2173–2190.
[23] J. Bosse, W. Götze, M. Lücke, Mode-coupling theory of simple classical liquids, Phys. Rev. A 17 (1) (1978) 434–454.
[24] C. Baysal, A. Atilgan, Relaxation kinetics and the glassiness of native proteins: coupling of timescales, Biophys. J. 88 (2005) 1570–1576.
[25] Y. Kamatari, H. Yamada, K. Akasaka, J. Jones, C. Dobson, L. Smith, Response of native and denaturated hen lysozyme to high pressure studied by 15N/1H NMR spectroscopy, Eur. J. Biochem. 268 (2001) 1782–1793.
[26] W. Doster, R. Gebhardt, High pressure—unfolding of myoglobin studied by dynamic neutron scattering, Chem. Phys. 292 (2003) 383–387.
[27] M.-S. Appavou, G. Gibrat, M.-C. Bellissent-Funel, Influence of pressure on structure and dynamics of bovine pancreatic trypsin inhibitor (BPTI): small angle and quasi-elastic neutron scattering studies, Biochim. Biophys. Acta 1764 (2006) 414–423.
[28] L. Meinhold, J. Smith, A. Kitao, A. Zewail, Picosecond fluctuating protein energy landscape mapped by pressure–temperature molecular dynamics simulation, PNAS 104 (44) (2007) 17261–17265.
[29] P. Bridgman, The coagulation of albumen by pressure, Proc. Am. Acad. Arts Sci. 49 (1914) 627–628.
[30] C. Balny, P. Masson, K. Heremans, High pressure effects on biological macromolecules: from structural changes to alteration of cellular processes, Biochim. Biophys. Acta 1595 (1–2) (2002) 3–10.
[31] M. Wang, G. Uhlenbeck, On the theory of Brownian motion II, Phys. Rev. 93 (1) (1945) 249–262.
[32] G. Kneller, Quasielastic neutron scattering and relaxation processes in proteins: analytical and simulation-based models, Phys. Chem. Chem. Phys. 7 (2005) 2641–2655.
[33] C. Gardiner, Handbook of Stochastic Methods, 2nd Edition, Springer Series in Synergetics, Springer, Berlin, 1985.
[34] N. van Kampen, Stochastic Processes in Physics and Chemistry, revised editionNorth Holland, Amsterdam, 1992.
[35] H. Risken, The Fokker–Planck Equation, 2nd Edition, Springer Series in Synergetics, Springer, Berlin, 1996.
[36] K. Oldham, J. Spanier, The Fractional Calculus, Academic Press, New York, 1974.
[37] M. Abramowitz, I. Stegun, Handbook of Mathematical Functions, Dover Publications, New York, 1972.
[38] A. Erdélyi, W. Magnus, F. Oberhettinger, F. Tricomi, Higher Transcendental Functions, McGraw Hill, New York, USA, 1955.
[39] P. Debnath, M. Wei, S. Xie, B. Cherayil, Multiple time scale dynamics of distance fluctuations in a semiflexible polymer: a one-dimensional generalized Langevin treatment, J. Chem. Phys. 123 (2005) 204903.
[40] V. Calandrini, D. Abergel, G. Kneller, Protein dynamics from a NMR perspective: networks of coupled rotators and fractional Brownian dynamics, J. Chem. Phys. 128 (14) (2008) 145102.
[41] M. Vaney, S. Maignan, M. RiesKautt, A. Ducruix, High-resolution structure (1.33 angstrom) of a HEW lysozyme tetragonal crystal grown in the APCF apparatus. data and structural comparison with a crystal grown under microgravity from spacehab-01 mission, Acta Cryst. D Biol. Cryst. 52 (1996) 505–517.
[42] H. Berman, J. Westbrook, Z. Feng, G. Gilliland, T. Bhat, H. Weissig, I. Shindyalov, P. Bourne, The Protein Data Bank, Nucleic Acids Res. 28 (2000) 235–242.
[43] K. Hinsen, G. Kneller, Projection methods for the analysis of complex motions in macromolecules, Mol. Sim. 23 (2000) 275–292.
[44] W. Cornell, P. Cieplak, C. Bayly, I.I.R. Gould, K. Merz, D. Ferguson, D. Spellmeyer, T. Fox, J. Caldwell, P. Kollman, A second generation force field for the simulation of proteins and nucleic acids, J. Am. Chem. Soc 117 (1995) 5179.
[45] H. Andersen, Molecular dynamics at constant pressure and/or constant temperature, J. Chem. Phys. 72 (4) (1980) 2384–2393.
[46] S. Nosé, A unified formulation of the constant temperature molecular dynamics methods, J. Chem. Phys. 81 (1) (1984) 511–519.
[47] G. Kneller, Superposition of molecular structures using quaternions, Mol. Sim. 7 (1991) 113–119.
[48] G. Kneller, Comment on "using quaternions to calculate RMSD" [J. Comp. Chem. 25, 1849 (2004)], J. Comp. Chem. 26 (15) (2005) 1660–1662.
[49] B. Nystrom, J. Roots, Quasielastic light scattering studies of the pressure-induced denaturation of lysozyme, Makromol. Chem. 185 (1984) 1441–1447.
[50] C. Gripon, L. Legrand, I. Rosenman, O. Vidal, M. Robert, F. Boué, Lysozyme–lysozyme interactions in under- and super-saturated solutions: a simple relation between the second virial coefficients in H_20 and D_2O, J. Crystal Growth 178 (1997) 575–584.
[51] M.-C. Bellissent-Funel, L. Bosio, A neutron scattering study of liquid D_2O under pressure and at various temperatures, J. Chem. Phys. 102 (9) (1995) 3727–3735.
[52] L. Meinhold, D. Clement, M. Tehei, R. Daniel, J. Finney, J. Smith, Protein dynamics and stability: the distribution of atomic fluctuations in thermophilic and mesophilic dihydrofolate reductase derived using elastic incoherent neutron scattering, Biophys. J. 94 (2008) 4812–4818.
[53] L. van Hove, Correlations in space and time and born approximation in systems of interacting particles, Phys. Rev. 93 (1) (1954) 249–262.